FATIGUE CRACK GROWTH OF CIRCULAR PIPES AND MODELLING OF SINGLE-EDGE-NOTCH TENSION (SENT) SPECIMEN

A THESIS SUBMITTED IN PARTIAL FULFILLMENT OF THE REQUIREMENTS FOR THE DEGREE OF

BACHELOR OF TECHNOLOGY

IN

MECHANICAL ENGINEERING

By:

SARTHAK SAMBIT SINGH 107ME066

SHANTANU PATNAIK 107ME057

SURAJ TRIPATHY 107ME020

DEPARTMENT OF MECHANICAL ENGINNERING

NATIONAL INSTITUTE OF TECHNOLOGY

ROURKELA – 769008

FATIGUE CRACK GROWTH OF CIRCULAR PIPES AND MODELLING OF SINGLE-EDGE-NOTCH TENSION (SENT) SPECIMEN

A THESIS SUBMITTED IN PARTIAL FULFILLMENT OF THE REQUIREMENTS FOR THE DEGREE OF

BACHELOR OF TECHNOLOGY

IN

MECHANICAL ENGINEERING

By:

SARTHAK SAMBIT SINGH 107ME066

SHANTANU PATNAIK 107ME057

SURAJ TRIPATHY 107ME020

Under the guidance of

Prof. P.K.Ray and Prof. B.B.Verma

DEPARTMENT OF MECHANICAL ENGINNERING

NATIONAL INSTITUTE OF TECHNOLOGY

ROURKELA – 769008

NATIONAL INSTITUTE OF TECHNOLOGY ROURKELA

CERTIFICATE

This is to certify that the thesis entitled **"**Fatigue Crack Growth of Circular Pipes and Modeling of Single-Edge-Notched Tension (SENT) Specimen**"** submitted by Sarthak Sambit Singh (Roll No. 107ME066), Shantanu Patnaik (Roll No. 107ME057) and Suraj Tripathy (Roll No. 107ME020) in the partial fulfillment of the requirements for the award of Bachelor of Technology degree in Mechanical Engineering at National Institute of Technology, Rourkela (Deemed University) is an authentic work carried out by them under our supervision and guidance.

To the best of our knowledge, the matter embodied in the thesis has not been submitted to any other University/Institute for the award of any Degree or Diploma.

Date:

Prof. P.K.Ray Prof. B.B.Verma

ACKNOWLEDGEMENT

We wish to express our deep sense of gratitude and indebtedness to **Prof. P.K.Ray,** Department of Mechanical Engineering and **Prof. B.B.Verma**, Department of Metallurgical and Materials Engineering, N.I.T Rourkela, for introducing the present topic and for their inspiring guidance, constructive criticism and valuable suggestion throughout this project work.

We also extend our sincere thanks to all our friends who have patiently helped us in accomplishing this undertaking. We also thank Mr. Shashi Kumar and Mr. Pawan Kumar for their constant support throughout the project work.

Place:

Date:

Sarthak Sambit Singh (107ME066)

Shantanu Patnaik (107ME057)

Suraj Tripathy (107ME020)

Department of Mechanical Engineering

National Institute of Technology

Rourkela - 769008

CONTENTS

LIST OF TABLES

LIST OF FIGURES

ABSTRACT

Pipe installations usually experience high amplitude Seismic Vibrations. These vibrations may initiate a new cracks or it may extend the severity of the exiting cracks. The monitoring of crack growth and propagation becomes essential if the installation of pipes carry a hazardous fluid. The compliance technique is one of the most commonly used methods to measure the crack growth in small size specimen used to monitor crack. Compact tension (CT), three point bend bar (TPBB) etc. are generally preferred for laboratory tests. Correlations are available for CT, TPBB and some other geometry of small laboratory specimens. However, for pipes and elbows no such correlations are available. Fatigue crack growth tests were carried out on a test specimen in Instron 8502 machine and the necessary data and graphs were analyzed. Fracture toughness analysis is done with the help of Scanning Electron Microscope (SEM).

The fatigue crack growth in a body is Exponential in nature. In the second part of this project a modified gamma model has been proposed to predict the crack growth in a Single Edge Notched Tension (SENT) Specimen. The values of the different parameters were obtained and the analysis was done after coding different programs in C++ and MATLAB software. The final result obtained was found to be coherent with the experimental findings.

CHAPTER 1

INTRODUCTION

FATIGUE

FRACTURE

NEED FOR MODELING CRACK GROWTH

1.1 FATIGUE

According to ASTM, Fatigue is defined as "the process of progressive localized permanent structural change occurring in a material subjected to conditions that produce fluctuating stresses at some point or points and that may culminate in cracks or complete fracture after a sufficient number of fluctuations."[8] The stress value in case of fatigue failure can be less than ultimate tensile stress and may be below yield stress limit of the material. Generally, fatigue loading implies to variation of stress and strain in a component in a cyclic manner. Most of the mechanical components experience fluctuating load due to change in:

- Load Magnitude
- Load Direction
- Load application point

Stages of fatigue failure are [7]:

1. **Crack Initiation** – It occurs in where there are localized stress concentrations and geometrical discontinuities are the places where it originates. In such places, the stress that is induced goes well above the local yield strength of the material.
2. **Crack Propagation** – Crack propagation occurs along grains or grain boundaries due to further increase in stress levels. With increase in crack size, cross sectional area resisting stress decreases.
3. **Fracture** – The area becomes insufficient to resist induced stress and results in failure of the component.

Factors that affect fatigue are [7]:

- **Cyclic stress state**: One or more properties of the stress state need to be considered, depending on the complexity of the geometry and the loading, such as stress amplitude, mean stress, biaxiality, in-phase or out-of-phase shear stress, and load sequence.
- **Geometry**: Notches and cross section area variations throughout a body are the places that have stress concentrations where fatigue cracks initiate.
- **Surface quality**: Surface roughness is the cause of microscopic stress concentrations and it lowers the fatigue strength

- **Material Type**: Fatigue life, as well as the behavior during cyclic loading, varies from one material to other, e.g. composites and polymers differ significantly from metals.
- **Residual stresses**: High levels of tensile residual stress can be produced from Welding, cutting, casting, and other manufacturing processes involving heat or deformation, which decreases the fatigue strength.
- **Size and distribution of internal defects**: Various casting defects like as gas porosity, non-metallic inclusions and shrinkage voids significantly reduces fatigue life of material.
- **Direction of loading**: Fatigue strength also depends on the direction of the principal stress in non-isotropic materials.
- **Grain size**: Generally smaller grains yield higher fatigue life, but the presence of various surface defects or scratches will have a higher influence than in a coarse grained alloy.
- **Environment**: Environmental conditions lead to erosion, corrosion, or gas-phase embrittlement, which affects the fatigue life of a component.
- **Temperature**: Extreme temperatures can affect and reduce fatigue life of a component.

1.2 FRACTURE

It is the local separation of an object or material into two or more pieces under action of stress. They are generally of two types: brittle fracture and ductile fracture.

Brittle Fracture: Here there is no gross plastic deformation before fatigue. Here tensile stress acts normal to crystallographic plane due to which the fracture occurs by the cleavage.

Ductile fracture: In ductile fracture, before failure, extensive gross plastic deformation takes place. Here material pulls apart rather than cracking,.

Modes of Failure:

There are three modes of crack.
MODE I – It is the opening mode. Here tensile stress acts normal to the plane of crack.

MODE II – Sliding mode where shear stress acts parallel to the plane of crack and perpendicular to the crack front.

MODE III – Tearing mode where shear stress acts parallel to the plane of crack and parallel to the crack front.

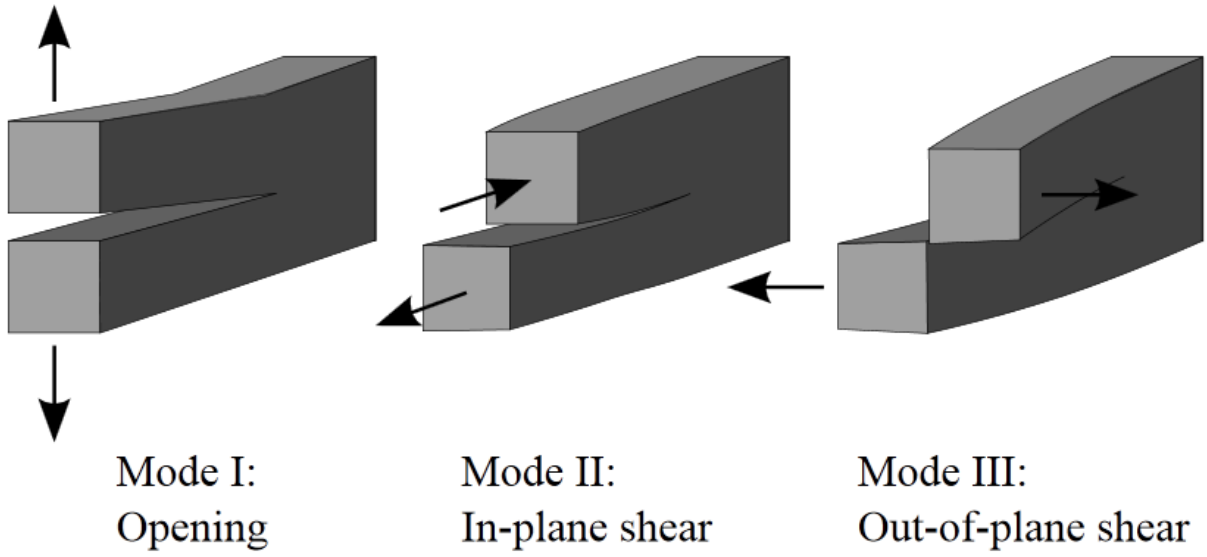

Fig. 1.1 Modes of Failure

1.3 NEED FOR MODELLING CRACK

Fatigue in material has been studied very closely in past century. 80 to 90 percent of the failure of materials is due to fatigue. Many infamous accidents like 'Versailles train crash' in 1848, 'de Havilland Comet passenger jets crash' in 1954, Alexander L. Kiel land oil platform capsize in 1980 were caused primarily due to fatigue failure[7]. Hence fatigue life prediction in components is considered highly important among engineers. Life of a component based on fatigue consists of two parts:

- No. of cycles after which crack initiates
- No. of cycles after which crack becomes unstable

The initiation of crack can be predicted from stress history and stress analysis but after crack initiation it becomes difficult to predict the no. of cycles after which the crack becomes unstable. Practical approach to predict crack is destructive in nature. It is also time consuming and accurate prediction of crack requires capital as well as skill. Thus to simplify crack prediction various models like Paris Model, Newman's model, Walker FCGR model, Forman model are proposed. Generally FEM analysis is used to predict crack growth. Here we use an empirical formula to predict FCGR in a SENT specimen without using complex FEM.

CHAPTER 2

LITERATURE REVIEW

2.1 CIRCULAR PIPES

2.1.1 ASSESSMENT OF PARTLY CIRCUMFERENTIAL CRACKS IN PIPES

This part of the project deals in predicting the stress intensity factor of a partly circumferential elliptical surface crack in pipes. Generally finite element analysis is used to determine stress intensity factor. Sometimes other approaches like line-spring models are used for a prediction of crack growth. However, the assessment by FEM is quite complicated as creation of fine meshes becomes cumbersome in 3D models. The line-spring element technique proposed by Rice and Levi (1972) [1] provide a simpler solution but it suffers from issues like correctly estimating Stress Intensity Factor in complex geometries. There are indirect methods where there is no need to develop a model that includes a crack. It reduces model development time and degrees of freedom.

Methods like conformal transform (C.D. Wallbrink *et al*.,2003)[2] can be used to analysis complex circumferential crack problem and rapidly solves partly circumferential cracks in pipes. This can be used to solve problems involving non-linear stress distributions. It can also solve problems involving double curvature, internal cracks quite accurately.

Here two coordinate systems are introduced and are defined as the ω-plane and the z-plane, respectively. The ω-plane describes the geometry of the (actual) cracks under investigation in the initial coordinate system. The z-plane basically describes the geometry where a known solution exists. Here two planes are related by equation

$$\omega = f(z) = e^{z} = re^{i\theta} \qquad (2.1)$$

where, r and θ are coordinates in w-plane.

With this equation the parameters of the problem in the ω-plane are related to those in the z-plane and by a set of transformations the stress intensity factor is found. The solution can then be corrected to account for the influence of the boundaries near the crack. Quite simply the above methodology can be expressed as:

$$K_I = K_I^{\infty} F_{\rho} \qquad (2.2)$$

Here K_I^{∞} is the infinite body solution developed by Vijayakumar and Atluri(1981)[3], and F_ρ is a modification factor used to correct the solution resulting from the inter-actions of the boundaries around the crack.

2.1.2ASSESSMENT OF STRESS INTENSITY FACTORS IN TUBULAR MEMBERS.

Stress Intensity Factor at the crack tip is a governing factor that influences fatigue crack propagation and helps in estimating residual life and criticality of the specimen. FEM technique uses Stress Intensity Factor for analyzing crack. But there are methods where crack need not be modeled explicitly (Peng *et. Al*) (2003)[5]. Majority of analysis for the prediction of fatigue cracking is based on line-spring models and finite element models. Solutions based on line-spring model only concern thin walled structures and do not consider complex loading while analyzing Stress intensity factors across the crack. Another approach based on conformal transformation can be used to calculate the Stress Intensity Factors for 3D cracks under arbitrary loading. But this method cannot be applied to solve problems that contain axial part through surface cracks. This uses exponential function to simplify the problem and develops a function to predict crack easily.

2.2 SINGLE EDGE NOTCHED TENSION (SENT) SPECIMEN

2.2.1 ASSESSMENT OF CRACK GROWTH IN SENT SPECIMEN.

Crack prediction in SENT specimen can be done by Finite Element Method as well as by use of compliance technique. The relationship can be expressed in form of a polynomial equation (A. Joni *et al.*,2006)[4]. The coefficients in the polynomial can be calculated from software like MATLAB. Analytically the coefficients can also be predicted using FEA software like FRANC2D. The results can be compared to get better crack estimates.

The relationship between compliance (deflection per unit load) and crack length is given in the form of a polynomial equation and is given by :

$$\frac{a}{w} = \sum_{i=0}^{i=5} C_i * U_x^i \quad (2.3)$$

where, C_i are the compliance coefficients which have to be determined by performing tests experimentally and also analytically by using FRANC2D and finally the results are compared. The general formula used in calculation of crack length is:

$$a/w = C_0 + C_1U + C_2U^2 + C_3U^3 + C_4U^4 + C_5U^5 \quad (2.4)$$

Where $C_0, C_1, \ldots$ are coefficients to be calculated

$$\text{And } U = (1 + (Evb/p)^{0.5})^{-1} \quad (2.5)$$

Where, E = Modulus of Elasticity

v = Linear Load Displacement

b = Thickness of Specimen

p = Load Applied

2.2.2 PREDICTION OF FATIGUE CRACK GROWTH AND RESIDUAL LIFE USING AN EXPONENTIAL MODEL

Earlier various efforts were adopted to correlate and develop relationship between fatigue crack growth and loading conditions. Mohanty *et. al* (2009)[6] proposed an exponential model to predict fatigue crack growth in structures/components subjected to cyclic loading. It takes into account the change in stress intensity factor which changes with extension of crack. It uses an equation called law of growth. It has a parameter called specific growth rate which depends on various loading conditions. Fatigue crack growth behavior is strongly dependent on initial crack length and load history. The value of specific crack growth rate, *m* increases incrementally and depends on two crack driving forces ΔK and K_{max} and material parameters K_C, E, σ_{ys}. The value of specific crack growth rate depends on a polynomial function of a parameter whose value is determined by material and loading conditions. The exponential model predicts crack propagation without complex numerical integration. It is valid for both stage II and stage III of fatigue crack propagation. The accuracy of the 'Exponential model' is much better than other available empirical models and the curves.

The general formula is given by :

$$a_j = a_i \, e^{(N_j - N_i) m_{ij}} \tag{2.6}$$

and,

$$m_{ij} = \frac{\ln \frac{a_j}{a_i}}{(N_j - N_i)} \tag{2.7}$$

where a_i and a_j is the crack length in i_{th} step and j_{th} step in *mm*, respectively; N_i and N_j is number of cycles in i_{th} step and j_{th} step, respectively; m_{ij} is specific growth rate in the interval *i–j*; *i* is the number of experimental steps and $j = i + 1$.

CHAPTER 3

EXPERIMENTAL DETAILS

SETUP AND DETAILS

MATERIAL PROPERTIES

3.1 SETUP AND DETAILS

Three straight circular through walled pipes with dimensions given below were considered for experimental work. The pipe material was preferably SEAMLESS PIPE OF ASTM A 312 TP 316L grades of steel which have in-plane crack growth. The tests were carried out on an Instron 8502 machine with 250 kN load capacity. The machine was also interfaced to a computer for control and data acquisition. The tests were conducted in air and in room temperature. Test on pipe were done by loading it under four point bending. Loading was up to large scale plastic deformation. The outer circumference of the pipe where the notch was made was marked by a marker at distance of 0.5mm distance between the markings. Also there was periodic significant unloading so as to create a beach mark on the crack surface. After the test, the crack surface was broke open and exact crack length was measured at various loading stages. The experiments considered in this study were conducted using the four-point bend method schematically shown in Figure 3.1.

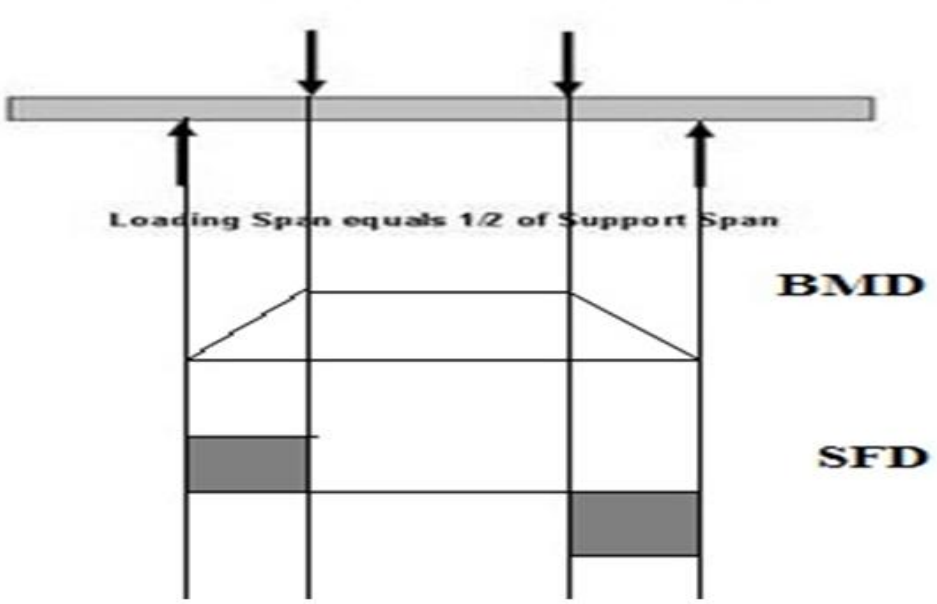

Fig. 3.1 Shear Force and Bending Moment Diagram for Four Point Bend Test

During the test the load was quasi-statically increased under displacement control, until the maximum load was reached. Because of the low compliance of the test rig, unstable crack propagation never occurred.

The test specimen was gripped between rollers on the INSTRON machine. This type of loading ensured that the notched section of the pipe was subjected to pure bending stress as only point contact was on the surfaces of two circles. The pipes with part through and through-wall notches were fatigue pre-cracked before the fracture tests to ensure sharpness of the crack tip. The pre-cracking was mainly done using a hack-saw and the wire EDM. This is shown in Figure 3.2

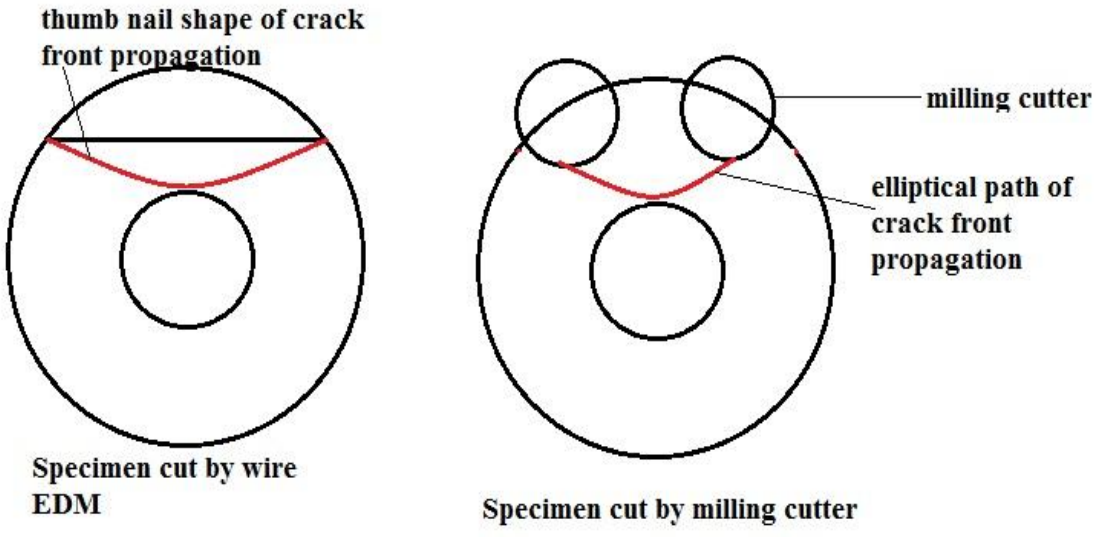

Fig. 3.2 Pre-Cracking of Specimens

Thereafter fracture tests were carried out on through-wall cracked pipes. The final through-wall crack size after the fatigue pre-cracking was taken as the initial crack size for the fracture tests. Pipes were subjected to static loading with a loading displacement rate of 0.036 $mm.s^{-1}$. During the test on through-wall cracked pipes, load line displacement (LLD), load and crack mouth opening displacement (CMOD) were recorded. During the tests on part-through cracked pipes, the crack depth along the notch length was measured using a micro gauge based on the principle of alternating current potential difference (ACPD), until the crack reached through thickness. Thereafter all the parameters measurement required for through-wall cracked pipe test was carried out. The test was carried out as per the guidelines of ASTME1820.Here the specimen is unloaded after every 1mm propagation of crack. Here the amplitude of loading was maintained constant all throughout the test. After certain number of cycles the pipe broke apart.

3.2 MATERIAL PROPERTIES

Tensile tests are done on specimens which were fabricated from the straight pipe. From these tests, tensile data (e.g. stress-strain diagram, yield stress, UTS, % elongation, % reduction in area and Young's modulus) were determined to be as follows:

UTS = 611.46 MPa

2/3 YS = 241.56 MPa

Also the pipe dimensions were as follows:

Extruded Diameter = 55mm

Outer Diameter (D_o) = 60mm

Inner Diameter (D_i) = 42mm

Thickness = 8mm

Length = 505mm

Shoulder Length = 53mm

Outer Span = 465mm

Inner Span = 205mm

Table 3.1 Load and Stress Intensity Factor Calculation

ΔK	ΔP	P_{mean}
25	8.61147	5.2625
30	10.35	6.325
35	12.078	7.381
40	13.797	8.4315
45	15.497	9.47042
50	17.2189	10.5522
55	18.940	11.5749
60	20.662	12.794
65	22.384	13.6794
70	24.1065	14.7317
75	25.8284	15.78403
80	27.5503	16.8363
85	29.2722	17.8885
90	30.9941	18.94084
95	32.716	19.99311
100	34.4379	21.0453

The figure shown here gives us an idea of how the circular pipe specimen is loaded in the Instron 8502 Machine and the final appearance of the circular pipe specimen after the fatigue failure.

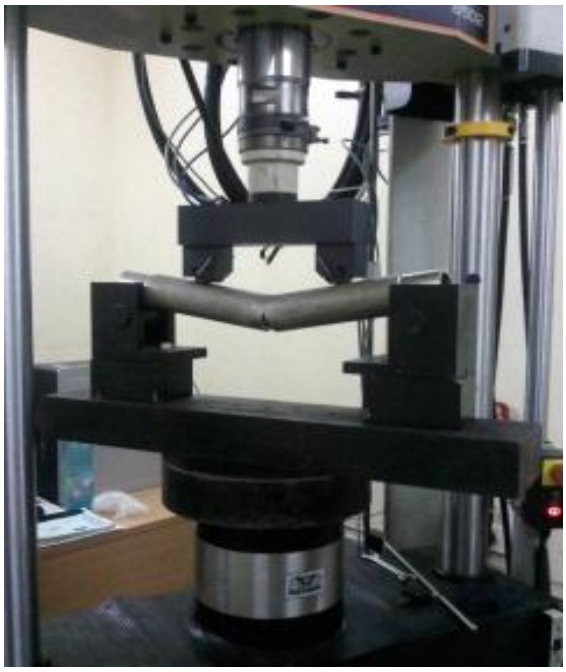

Fig.3.3 Instron 8052 with circular specimen

Fig. 3.4 The final cracked circular specimen

The figure shown here gives us an idea of how the circular pipe specimen is loaded in the Instron 8502 Machine

Fig. 3.5 Instron 8052 with SENT specimen

CHAPTER 4

FORMULATIONS OF THE MODEL

EXPERIMENTAL PROCEDURE

MODEL FORMULATION

4.1 EXPERIMENTAL PROCEDURE

The present study deals with life prediction model in 7020 and 2024 Al-alloys. The 7020 alloy was subjected to T7 heat treated condition whereas 2024 alloy was subjected to T3 heat treated condition in order to obtain optimum mechanical properties. The chemical and physical properties of the two alloys are given in the tables below:

Table 4.1 Chemical Composition of 7020-T7 and 2024-T3 Al Alloys

Materials	Al	Cu	Mg	Mn	Fe	Si	Zn	Cr	Others
7020-T7 Al-Alloy	Main Constituent	0.05	1.2	0.43	0.37	0.22	4.6	-	-
2024-T3 Al-Alloy	90.7-94.7	3.8-4.9	1.2-1.8	0.3-0.9	0.5	0.5	0.25	0.1	0.15

Table 4.2 Mechanical Properties of 7020-T7 and 2024-T3 Al Alloys

Material	Tensile Strength (σ_{ut}) MPa	Yield Strength (σ_{ys}) MPa	Young's Modulus (E) MPa	Poisson's Ratio (v)	Plane Strain Fracture Toughness (K_{1C}) MPa$\sqrt{m}$	Plane Stress Fracture Toughness (K_C) MPa$\sqrt{m}$	Elongation
7020-T7 Al-Alloy	352.14	314.7	70000	0.33	50.12	236.8	21.54% in 40mm
2024-T3 Al-Alloy	469	324	73100	0.33	37	95.31	19% in 12.7mm

SENT specimens were used to conduct the experiment. The Fig. 4.1 shows the detailed geometry of the specimen. The experiments were performed on Instron 8502 machine with 250 kN load cell capacity and which is interfaced to a computer for data acquisition and control. The tests were conduction in normal atmospheric air and at room temperature. The test specimens were pre-cracked under mode-I loading to *a/w* ratio of 0.3. They were then

subjected to constant load test with progressive increase in ΔK with crack extension, maintaining a load ratio of 0.1. The load cycles were applied at a frequency of 6 Hz which are in sinusoidal form. The crack growth was monitored using a crack opening displacement (COD) gauge mounted on the face of the notch.

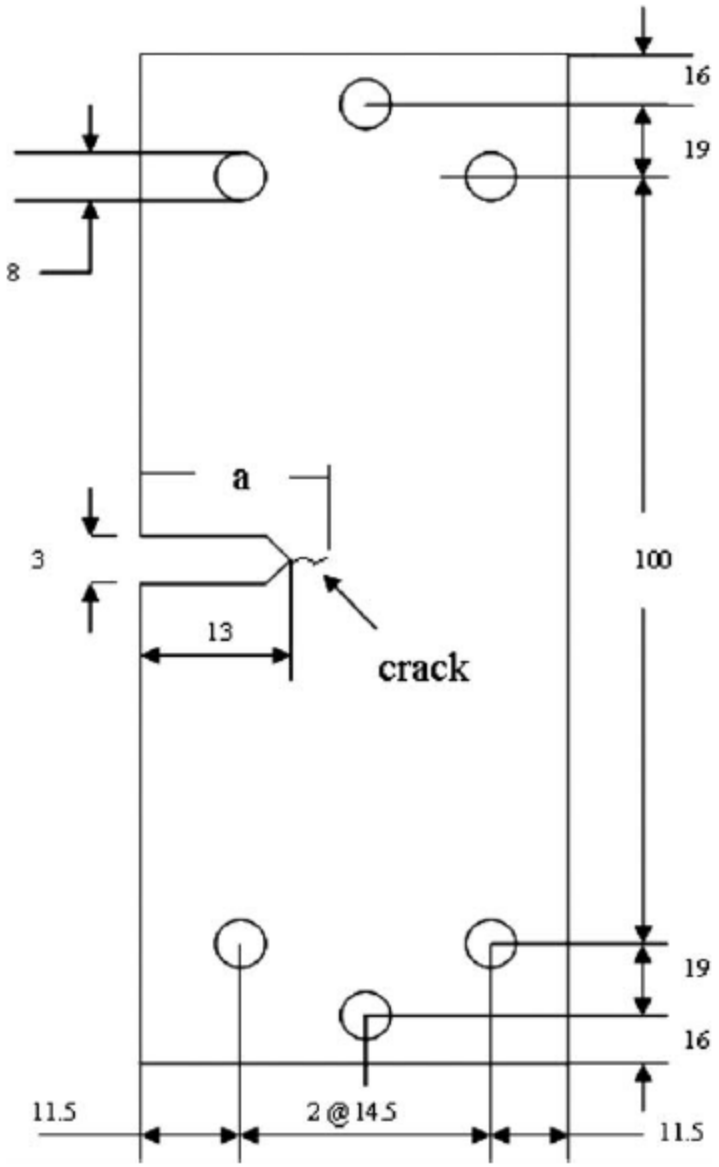

Fig 4.1 Single edge notched specimen geometry [4]

The crack length was plotted against the number of cycles the specimen endured. Also the stress intensity factor range was plotted against the crack growth rate (*da/dN*). These values were measured by the COD gauge analyzing the stress level and were interfaced to the computer to generate us the graphs for the two alloys.[6]

For the Al 7020-T7 alloys the graph showing the variation of crack length with the number of cycles is plotted below:

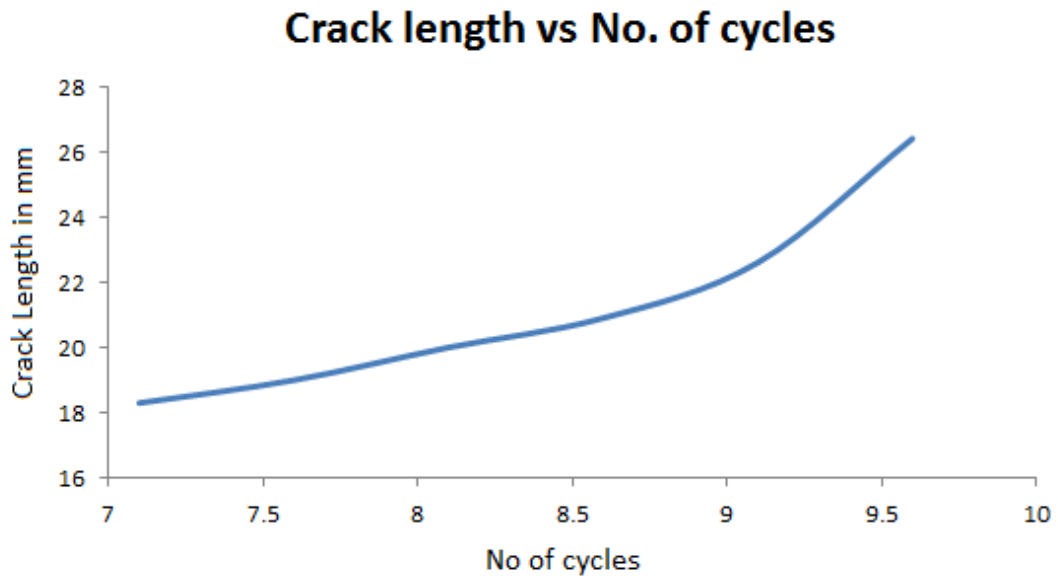

Fig 4.2 Crack Length vs. No. of Cycles for Al 7020-T7 [6]

From the above graph, the following tables were reconstructed for Al7020-T7 alloys:

Table 4.3 Crack Length vs. No. of Cycles for Al 7020-T7[6]

Number of Cycles N (x 10^4)	***Crack Length (mm)***
7.1	18.3
7.6	19.0
8.1	20.0
8.6	20.9
9.1	22.6
9.6	26.4

The following graph were plotted for Al 7020-T7 alloys between delta *K* and *da/dN*

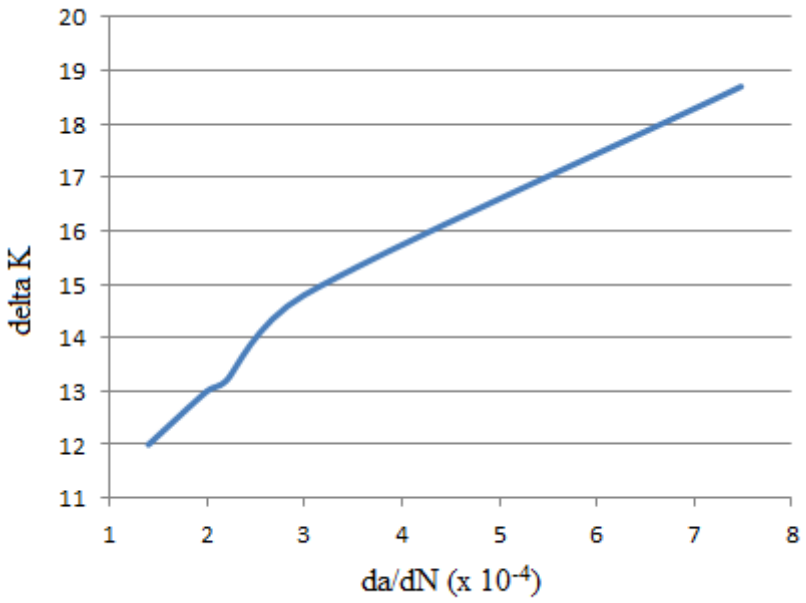

Fig 4.3 delta *K* vs. *da/dN* for Al 7020-T7 [6]

From the above graph, the following tables were reconstructed for Al 7020-T7 alloys:

Table 4.4 delta *K* vs. *da/dN* for Al 7020-T7 [6]

Stress Intensity Factor ΔK ***(MPa.m$^{0.5}$)***	***Crack Growth Rate (da/dN) (x 10^{-4}) (mm/cycle)***
12	1.4
13	2.0
13.2	2.2
14.8	3.0
18.7	7.48

For the Al 2024-T3 alloys the graph showing the variation of crack length with the number of cycles is presented in Fig. 4.3

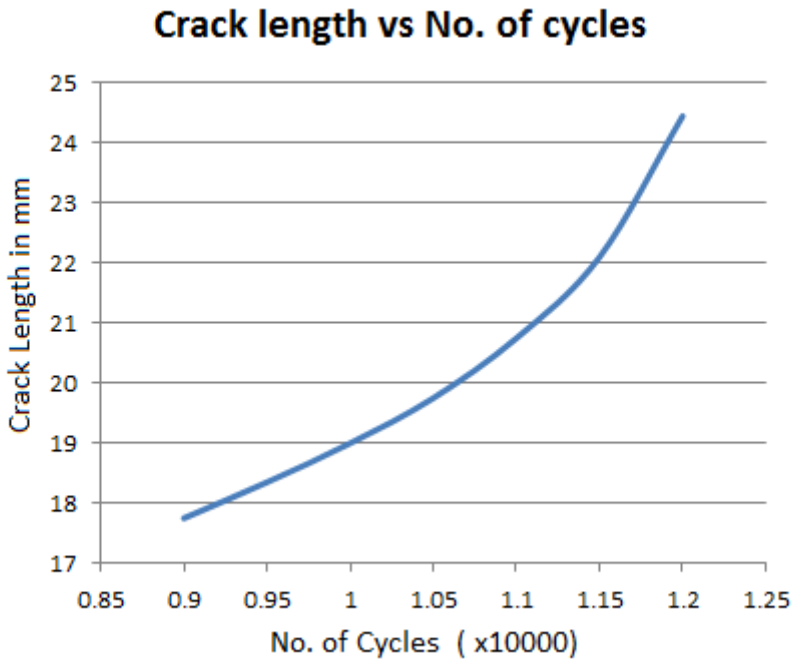

Fig 4.4 Crack Length vs No. of Cycles for Al 2024-T3 [6]

From the above graph, the following tables were reconstructed for Al 2024-T3 alloys:

Table 4.5 Crack Length vs. No. of Cycles for Al 2024-T3 [6]

Number of Cycles N (x 10^5)	Crack Length (mm)
0.9	17.75
0.95	18.35
1.0	19.0
1.05	19.75
1.10	20.75
1.15	22.10
1.20	24.45

The following graph were plotted for Al 2024-T3 alloys between delta *K* and *da/dN*

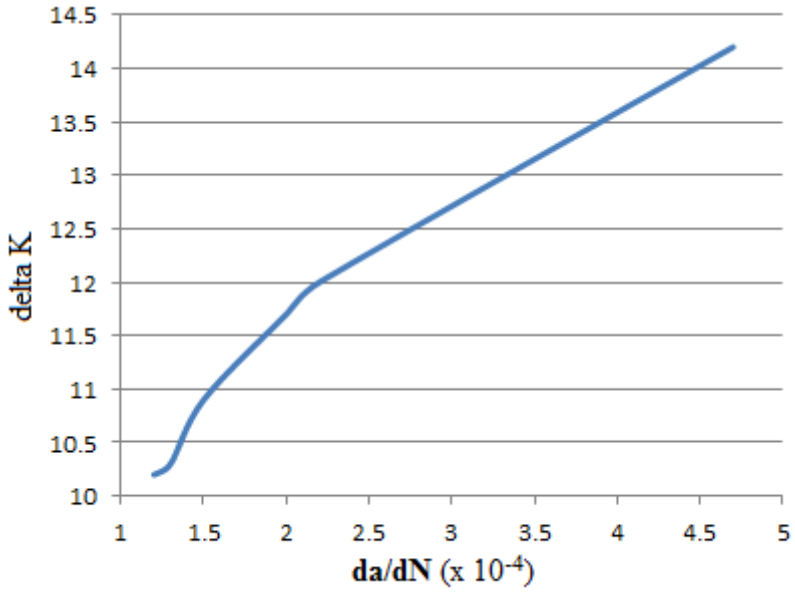

Fig 4.5 delta *K* vs. *da/dN* for Al 2024-T3 alloy [6]

From the above graph, the following tables were reconstructed for Al 2024-T3 alloys

Table 4.6 delta *K* vs. *da/dN* for Al 2024-T3 alloy [6]

Stress Intensity Factor ΔK(MPa.$m^{0.5}$)	Crack Growth Rate (da/dN) (x 10^{-4}) (mm/cycle)
10.2	1.2
10.3	1.3
10.9	1.5
11.7	2.0
12.0	2.2
14.2	4.7

4.2 MODEL FORMULATION

Gamma function is a variant of factorial function with its arguments shifted by 1. That is if 'n' is a positive integer then:

$$\Gamma(n) = (n-1)! \tag{4.1}$$

The Gamma function is defined for every complex number whose real part is positive and greater than zero. Generally it is given by an integral as mentioned below:

$$\Gamma(z) = \int_0^\infty t^{z-1} e^{-t}\,\mathrm{d}t\,. \quad , \text{Re(z) } >0 \tag{4.2}$$

proposed model is a modification of the Gamma function.

Here *t* can be approximated as number of cycles *N*. The parameter *z* was chosen in such a way that it becomes a non-dimensional parameter yet representing the properties that affect crack growth.

Here since the integral is finite the value of integral is not *Γ(z)*. The integral was assumed to be equal to a non-dimensional representing crack growth at the end of fixed cycles of loading. Generally fatigue crack growth depends on the initial crack length material properties and dimensions, loading conditions etc. The non-dimensional parameter was chosen to include all those properties. So the formula for predicting the final crack length at the end of cycle is given as

$$\frac{ma_1}{w} = \int_0^N N^{(\frac{ma_0}{w}-1)} e^{-N} dN \tag{4.3}$$

Here *m* also a non-dimensional parameter whose value remain approximately constant for a given cycle interval. At first the value of *m* on RHS and LHS were considered different say m_1 on LHS and m_2 on RHS. The values of a_0, *w*, a_1, *N* were given as input is made fixed for a particular interval of cycles. The value of m_1 is input every time and value of m_2 was computed every time. The value of m_1 at which m_1 nearly becomes equal to 'm_2' was considered as the value of *m* for the interval.

$$\frac{m_2 a_1}{w} = \int_0^N N^{(\frac{m_1 a_0}{w}-1)} e^{-N} dN. \tag{4.4}$$

CHAPTER 5

RESULTS AND DISCUSSIONS

FOR CIRCULAR PIPES

FOR THE MODELING OF SENT SPECIMEN

5.1 RESULTS AND DISCUSSIONS FOR CIRCULAR PIPES

5.1.1 DATA FROM INSTRON MACHINE

Table 5.1 Results obtained from Instron machine for Pipe 1

Length (curve) mm	a (mm)	a/w ratio	Max. load(N)	Monitored Crack length (mm)	No. of Cycles	ΔK	EVB/P	Slope (x 10^{-6})
25.4	2.60	.28	38264	49.46	94195	275.318	569.18	1.2311
28	3.20	0.355	38310	50.92	117679	343.503	630.25	2.5232
34	4.58	0.508	38349	51.53	127741	383.876	692.15	2.7122
38.5	5.96	0.662	38356	52.09	133907	421.47	796.518	2.8311
42	7.05	0.783	38360	52.58	145880	466.66	907.196	3.2231
46	8.39	0.932	38360	53.199	151392	514.76	1080	3.2231

The above results were obtained from the computer interfaced to the Instron 8502 Machine. Using these values a general curve was plotted to show the variation of crack length with ΔK and with No. of Cycles, separately.

Table 5.2 Results obtained from Instron machine for Pipe 2

Length (curve) (mm)	a(mm)	a/w	Max. load	Monitored Crack length (mm)	No. of Cycles N	ΔK(MPa)	EVB/P	Slope (x 10^{-6})
27.5	3.096	0.344	38343	51.91	125876	408.722	756.665	2.6762
31.5	4.039	0.44	38304.4	52.33	4510	443.329	845.43	3.0051
35.5	5.096	0.566	38325	52.79	4399	486.89	962.5	3.4395
39.5	6.26	0.696	38304.1	53.28	4193	541.65	1128.32	4.5503
43.5	7.54	0.837	38377	53.71	3241	600.40	1289.31	5.1366
47.5	8.916	0.99	38351.6	54.07	2137	652.55	1452.7	5.737

The above results were obtained from the computer interfaced to the Instron 8502 Machine.

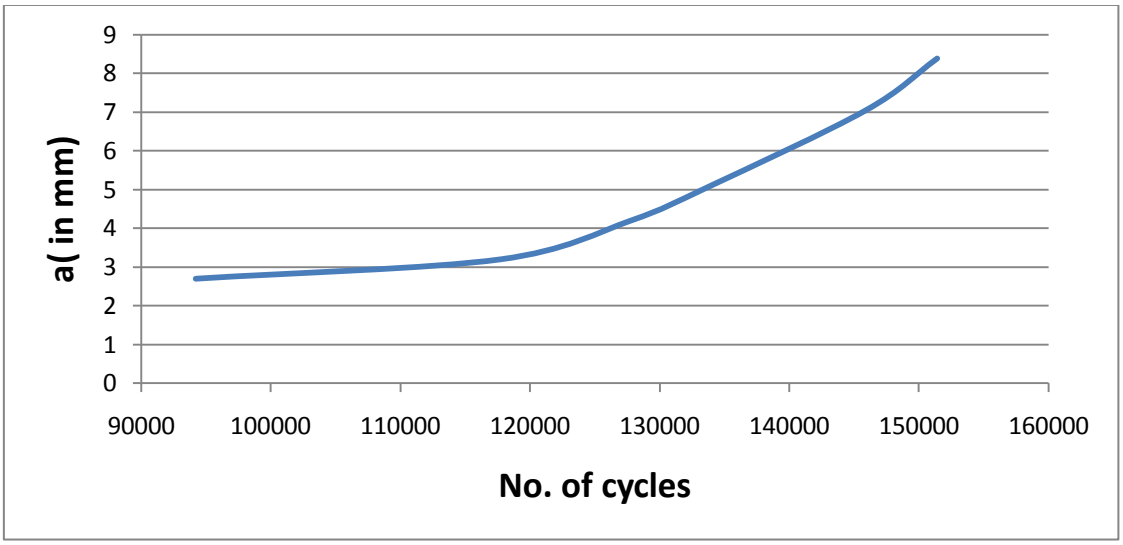

Fig. 5.1 *a* vs. No. of Cycles for pipe 1

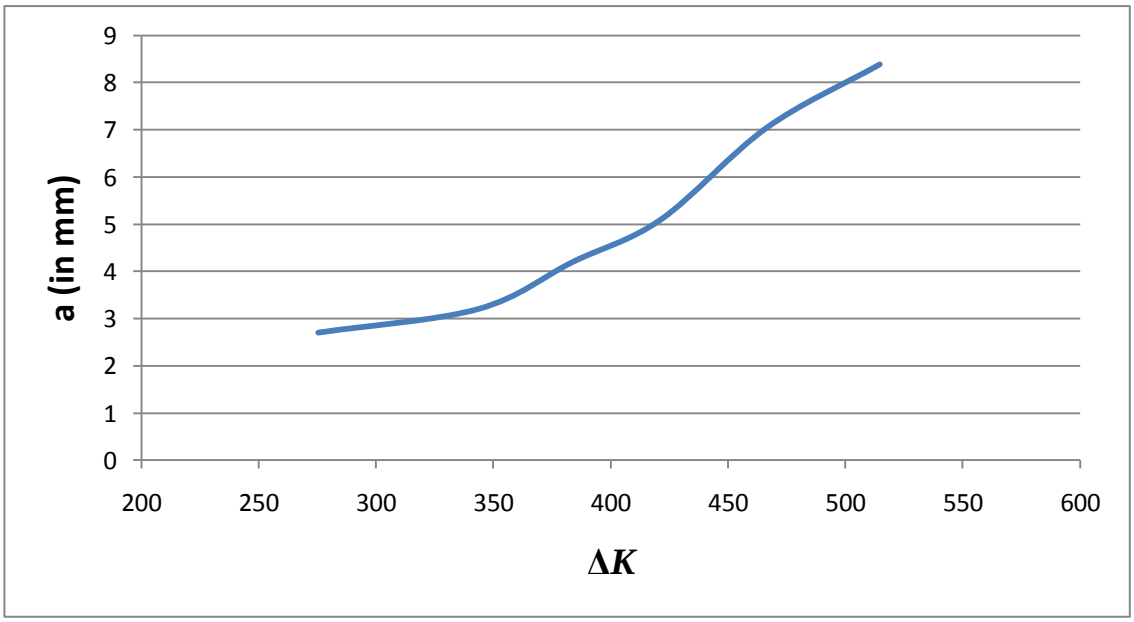

Fig. 5.2 *a* vs. Δ*K* for pipe 1

The transverse section of the circular pipe where the crack occurred was taken and viewed under Scanning Electron Microscope(SEM).Faintly appeared Beach Marks were seen under fracto--graph.

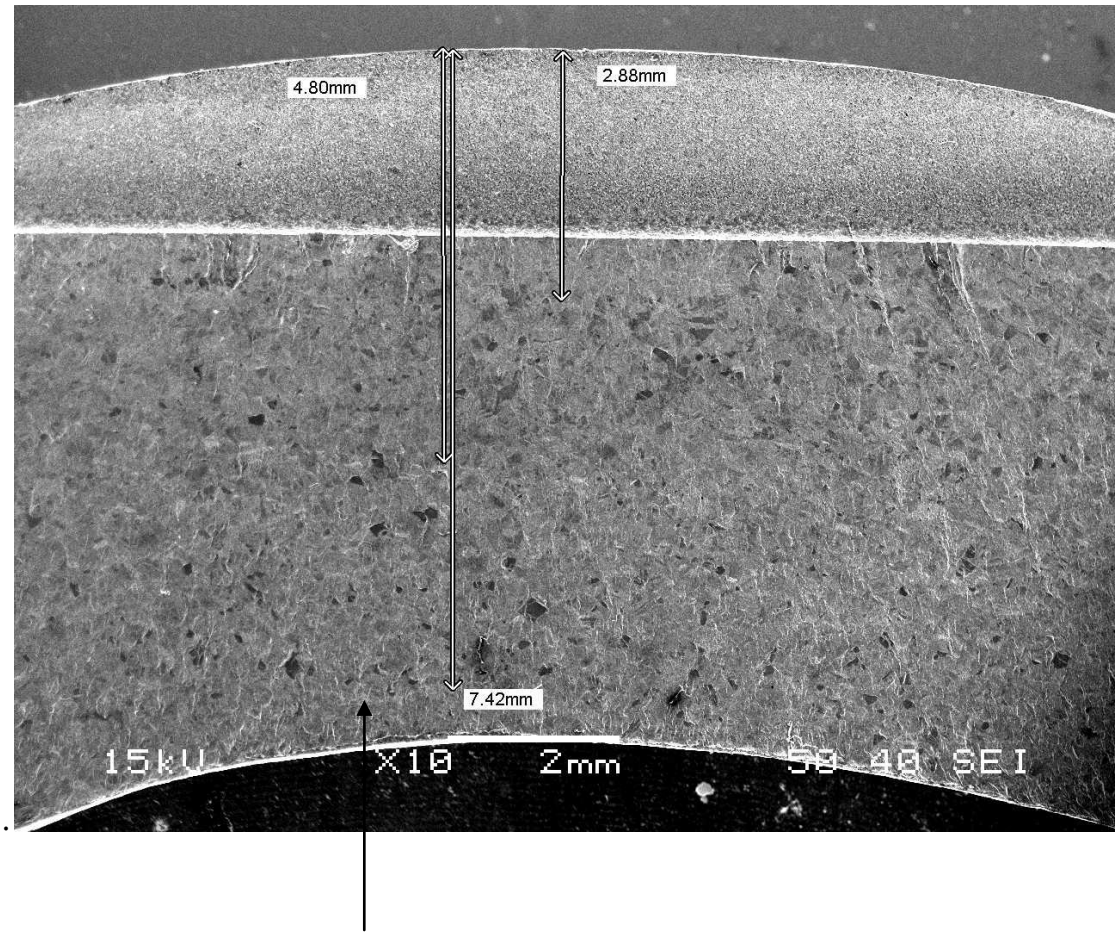

Faintly appeared beach mark

Fig.5.3

5.2 RESULTS AND DISCUSSIONS FOR THE MODELING OF SENT SPECIMEN

The following tables were constructed for Al 7020-T7 alloys:

Table 5.3 Values of *m* for Al 7020-T7

No. of Cycles(10^4)	**Crack Length (mm)**	***m* in Simpson's 1/3 rule**	**'m_1' from MATLAB**	**m_2 from MATLAB**
7.1	18.3			
7.6	19.0	10.248	10.249	10.253
8.1	20.0	9.9143	9.912	9.91
8.6	21.1	9.3963	9.436	9.429
9.1	22.6	9.0893	8.976	8.975
9.6	26.34	8.610	8.601	8.604

Table 5.4 Values of delta *K*, *da/dN* and *m* for Al 7020-T7

Crack Growth Rate *(da/dN)* (x 10^{-4}) (mm/cycle)	**Stress Intensity Factor ΔK (MPa.$m^{0.5}$)**	**The values of *m* from the empirical relation**
1.4	12	10.21
2.0	13	9.91
2.2	13.2	9.85
3.0	14.8	9.43
7.48	18.7	8.82

The following trends were observed when the graph was plotted for ‘m-model’ and ‘m-experimental’ with delta K for Al 7020-T7 alloy:

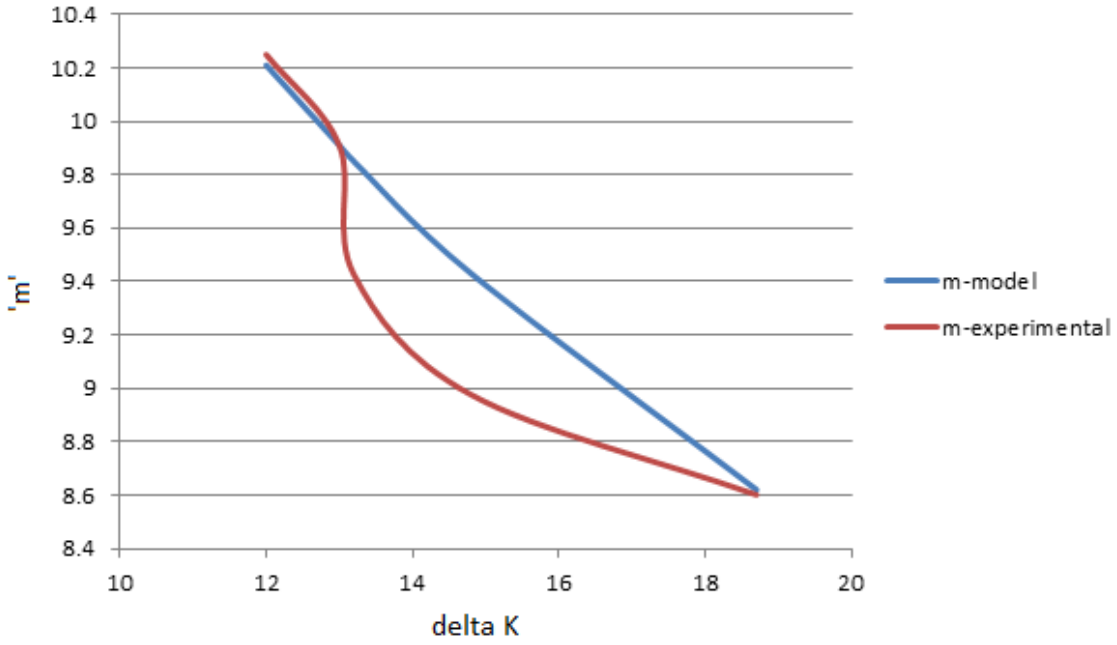

Fig 5.4 *m* vs. delta *K* for Al 7020-T7 alloy

Similarly the following tables were constructed for Al 2024-T3 alloys:

Table 5.5 Values of *m* for Al 2024-T3

No. of Cycles(10^5)	***Crack Length (mm)***	***‘m_1’ from MATLAB***	***‘m_2’ from MATLAB***
0.9	17.75		
0.95	18.35	10.551	10.551
1.0	19.0	10.211	10.211
1.05	19.75	9.876	9.876
1.10	20.75	9.532	9.532
1.15	22.10	9.112	9.112
1.20	24.45	8.657	8.657

Table 5.6 Values of delta *K*, *da/dN* and *m* for Al 2024-T3

Crack Growth Rate *(da/dN)* (x 10^{-4}) (mm/cycle)	**Stress Intensity Factor ΔK (MPa.$m^{0.5}$)**	**The values of *m* from the empirical relation**
1.2	10.2	9.87
1.3	10.3	9.84
1.5	10.9	9.6
2.0	11.7	9.33
2.2	12.0	9.21
4.7	14.2	8.57

The following trends were observed when the graph was plotted for *m*-model and *m*-experimental with delta K for Al 2024-T3 alloy:

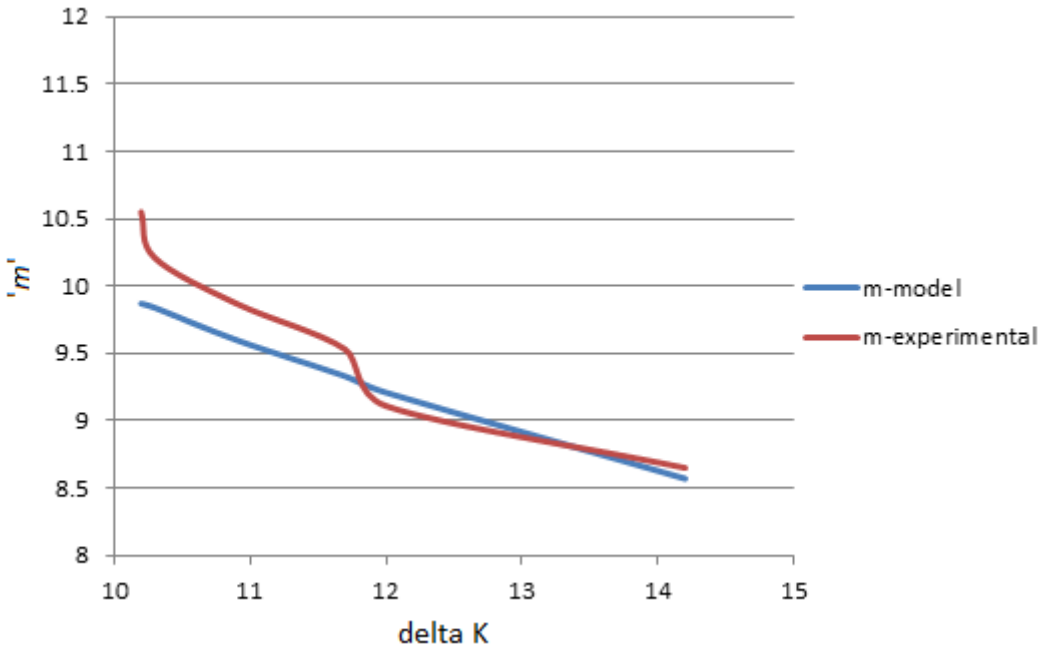

Fig 5.5 *m* vs. delta *K* for Al 2024-T3

From the above two tables the value of 'm' is found to have a reducing trend in both cases. The value of *m* reduces with increase in the value of Δ*K*. The value of m changes with change

in loading condition as well as crack length. Hence it was needed to correlate parameter *m* with parameters like two crack driving forces ΔK and K_{max} and with the material parameters such as plane stress fracture toughness (K_C), modulus of elasticity (E) and yield stress (σ_{ys}). Fatigue crack growth depends on both ΔK and K_{max} in order to consider effects of mean stress. Since the modeling covers region III the value of fracture toughness (K_C) has to be considered. Crack growth also depends upon the material parameters like yield stress (σ_{ys}) , Young's Modulus (E) and Ultimate strength (σ_{ut}) . The parameter 'm' is dimensionless and has a decreasing trend. So the value of *m* is correlated with dimensionless quantities like (E/ σ_{ys}), (K_C / ΔK), (K_{min} /K_{max}).

The resulting value of *m* is represented as:

$$m = \left(\frac{E}{\sigma_{ys}} \times \frac{K_c}{\Delta \mathrm{K}} \times \frac{K_{min}}{K_{max}}\right)^e \tag{5.1}$$

Here the value of exponent *e* varies from one material to other. The values of *e* for both the specimens used in the model are given below:

Table 5.7 Values of *e* for different material

Material	Exponent *e*
7020-T7 Al Alloy	0.382
2024-T3 Al Alloy	0.428

The value of *e* for each case as shown is different hence it must depend on certain properties which vary from one specimen to other. After some permutations it was found that the value of *e* depends upon the material parameters like ultimate strength (σ_{ut}) and the Young's (E) of the material. It was found that the ratio of the values of *e* depends upon the ratio:

$$e = \sqrt{\frac{\frac{\sigma_{ut2}}{E_2}}{\frac{\sigma_{ut1}}{E_1}}} \qquad (5.2)$$

The values of *e* were compared and calculated. It was found that the value of *e* satisfies following formula:

$$e = C\sqrt{\frac{\sigma_{ut}}{E_1}} \qquad (5.3)$$

Where C= Constant

Comparing this formula with the values of exponents in each case it was found that the value of *e* is approximately equals to:

$$e = 5.36\sqrt{\frac{\sigma_{ut}}{E_1}} \qquad (5.4)$$

CHAPTER 6

CONCLUSION

FOR CIRCULAR PIPES

MODELING OF SENT SPECIMEN

6.1 FOR CIRCULAR PIPES

1. From Fig. 5.1, it was observed that the crack growth rate increases very sluggishly initially with the no. of cycles but after that the crack growth rate increase at a faster rate.

2. From Fig. 5.1,it was observed that the crack growth rate increases very sluggishly initially with ΔK but after that the crack growth rate increase at a faster rate.

3. The transverse section of the circular pipe where the crack occurred was cut by means of a hand milling machine. It was cut in such a way that crack surface is not hampered. This section is then viewed under Scanning Electron Microscope (SEM) in order to see the pattern of Beach Marks. But no prominent beach marks were seen in the fracto-graph. The reason for this might be due to the fact that the specimen was subjected to constant amplitude loading with the growth/propagation of the crack. The possibility of the appearance of beach marks would have been more prominent if the specimen would have been subjected to increasing amplitude loading with the growth/propagation of the crack after every unloading.

6.2 MODELING OF SENT SPECIMEN

1. The Modified Gamma Model of the form,

$$\frac{ma_1}{w} = \int_0^N N^{(\frac{ma_0}{w}-1)} e^{-N} dN \qquad (6.1)$$

is used for predicting the fatigue life of a component without going for the numerical integration. This formula holds good in the region II and region III of the fatigue life curve. The results obtained from the Modified Gamma Model are in good agreement with the experimental results for the SENT specimen. The variation is primarily due to experimental errors or other errors arising due faulty reading and human error. This method can be extended to circular pipes and elbows. The value of '*m'* can be modified for use in prediction of crack for other non standard specimens. This method is easy to interpret and less time consuming in successfully predicting crack with good degree of accuracy.

2. There are many other method and models like Weibull Model, Beta Model that can be modified and adopted for predicting crack growth for different specimen

CHAPTER 7

REFERENCES

[1] Rice, J.R. and Levy, N. (1972). The part-through surface crack in an elastic plate. *Journal of Applied Mechanics, Transactions ASME*, 185–194.

[2] Wallbrink C.D., Peng D. and Jones R. (2003). Assessment of partly circumferential cracks in pipes. *International Journal of Fracture (2005)*: 167-181

[3] Vijayakumar, K. and Atluri, S.N. (1981). Embedded elliptical crack, in an infinite solid, subject to arbitrary crack-face tractions. *Journal of Applied Mechanics, Transactions ASME* 48, 88–96.

[4] Mohanty J.R. , Joni A. , Ray P.K. , Verma B.B. (2006). Determination of crack coefficients for a single edge-notch tension specimen using franc2d program. *Recent trends in mechatronics, nanotechnology and robotics RTMNR(2006)*,742-746

[5] Peng D., Wallbrink C., Jones R. (2004). An assessment of stress intensity factors for surface flaws in a tubular member. *Engineering Fracture Mechanics Volume 72, Issue 3, February 2005*, 357-371

[6] Mohanty J.R., Ray P.K. , Verma B.B. (2008). Prediction of fatigue crack growth and residual life using an exponential model: Part I (constant amplitude loading). *International Journal of Fatigue Volume 31, Issue 3, March 2009*, Pages 418-424

[7] *Wikipedia*, May 02 2011. < http://en.wikipedia.org/wiki/Fatigue_(material)>

[8] Stephens, Ralph I.; Fuchs, Henry O. (2001). *Metal Fatigue in Engineering* (Second edition ed.). John Wiley & Sons, Inc.. p. 69.

CHAPTER 8

APPENDIX

8.1 FOR CIRCULAR PIPES

In order to feed data to the INSTRON machine, via the computer, some calculations were done. A sample calculation is done below:

Assuming Stress Intensity Factor $\Delta K = 30$ MPa and Range R=0.1

Now, we know that $\Delta K = \Delta\sigma * (\pi * R * \theta)^{1/2} * F(\theta)$

where $F(\theta) = 1 + 6.8\,(\theta/\pi)^{3/2} - 13.6(\theta/\pi)^{5/2} + 20(\theta/\pi)^{7/2}$

Now here $2\theta = 90^0$ or $\theta = 45^0$

Therefore, $\theta/\pi = 0.25$ or $F(\theta) = 1.5812$

Radius $R = 21 \times 10^{-3}$ m

Therefore, $\Delta\sigma = 83.58$ MPa

But $\Delta\sigma = \sigma_{max} - \sigma_{min} = \sigma_{max}(1-R) = 0.9\,\sigma_{max}$

Or $\sigma_{max} = 92.86$ Mpa

$I = \pi/64\,(D_o^4 - D_i^4)$ and a = (465-205)/2 = 130 mm

$y = D_0/2$

Now $\frac{M}{I} = \frac{\sigma max}{y}$

or $\frac{P.a}{I} = \frac{\sigma max}{y}$

or $P = 0.115 \times 10^5$ N = 11.5 kN

$P_{min} = P_{max} * R = 1.15$ kN

$\Delta P = 10.35$ KN and $P_{mean} = 6.325$ kN

8.2 For Modeling of SENT Specimen

The value was computed with the help of software MATLAB as well as C++ where Simpson's 1/3 Rule was applied whose code is given in the table below.

```
//Program to calculate value of 'm'
#include<iostream>
#include<conio.h>
#include<math.h>
using namespace std;
int main()
{
      long double a1,w,m1,m2,a2,a,b,h,f,s0,s1,s2,a11;
      long double i,m;
      a1=18.3;          //initial crack length
      a2=19.0;          //final crack length
      a=0.0;
      b=5000;           //number of cycles
      w=52.00;          //value of width
      cout<<"\nEnter the value of m1 :";
      cin>>m1;          //Value of m1
      m=10000000;
      h=(b-a)/m;
      s1=0;
      s2=0;
      //Simpson's 1/3 rule computation
      s0=powl(a,((m1*a1/w)-1))*expl(-a)+powl(b,((m1*a1/w)-1))*expl(-
b);
      for (i=1.0;i<m;i+=2.0)
      {
            a11=a+i*h;
```

```
            s1=s1+powl(a11,((m1*a1/w)-1))*expl(-a11);
      }
      a11=0;
      for(i=2.0;i<m;i+=2.0)
      {
            a11=a+i*h;
            s2=s2+powl(a11,((m1*a1/w)-1))*expl(-a11);
      }
      f=(h/3)*(s0+4*s1+2*s2);
      m2=f*w/a2;
      cout<<"\nThe value of m2 is :"<<m2;
      return(0);
}
```

MATLAB sample program

```
syms x;

>> int((x.^2.607).*exp(-x),0,5000)

 ans =

(2542995543*gamma(607/1000))/1000000000 - (25013039189449*5000^(607/1000))/(1000000*exp(5000)) -
(2542995543*igamma(607/1000, 5000))/1000000000

 >> (2542995543*gamma(607/1000))/1000000000 - (25013039189449*5000^(607/1000))/(1000000*exp(5000))

 ans =    3.7467
```